17th World Conference on Earthquake Engineering, 17WCEE
Sendai, Japan - September 13th to 18th 2020

Including topographic effects in earthquake loss estimation - A comparative study

S. Molina[1], Lang, D.[2], Agea-Medina, N.[3], Galiana Merino, J.J.[4,7], Soler-Llorens, J.L.[1], Meslem, A.[5], Singh, Y.[6]

[1] *Dpt. of Earth and Environmental Science, University of Alicante, Spain, sergio.molina@ua.es, jl.soler@ua.es*
[2] *Natural Hazards, Norwegian Geotechnical Institute (NGI), Norway, dominik.lang@ngi.no*
[3] *Multidisciplinary Institute for Environmental Studies, University of Alicante, Spain, noelia.agea@gmail.com*
[4] *Dpt. of Physics, Systems Engineering and Signal Theory, University of Alicante, Spain juanjo@dfists.ua.es*
[5] *Dpt. of Applied Seismology, NORSAR, Norway, abdelghani@norsar.no*
[6] *Dpt. of Earthquake Engineering, Indian Institute of Technology Roorkee (IITR), India, yogendra.eq@gmail.com*
[7] *University Institute of Physics Applied to Sciences and Technologies, University of Alicante, Spain*

Abstract

Studies on the phenomenon of topographic amplification of seismic waves date back to the early 1960s. Since then, many studies have revealed that topographic features such as slopes, cliffs, hills or canyons are able to alter seismic ground motion significantly. Depending on which part of the topographic feature is considered, seismic ground motion can be either deamplified (i.e. weakened or suppressed) or amplified. The latter has been often observed at hilltops or close to ridges and thereby contributed to greater building damage. These effects have hence a significant impact on earthquake loss estimation. The review of a great number of studies on topographic amplification, both experimental and theoretical, shows that significant differences exist in the topographic amplification factors derived through the different approaches. The few seismic design code provisions addressing the topic of topographic amplification handle this issue in a very simplified way by basically adding a period-independent amplification factor when constructing the elastic design response spectrum. Therefore, a comparison between the damage results (in terms of Mean Damage Ratio – MDR) when using period-dependent topographic amplification relationships and the simplified factors provided by the Eurocode 8 and the Italian code are conducted. Those relationships compute the topographic amplification factor using a simplified hill geometry with parameters H (height of the hill), L (half width of the hill), and H/L (slope of the relief).

First, two sites are chosen at several distance from a hypothetical active fault (20 and 40 km epicentral distance) and three earthquakes (Mw 5.5, 6.0 and 6.5) are simulated through a ground-motion prediction equation. Using the software SELENA, MDR values are computed for varying topography relief (slope) ranges from 0 to 35º and varying soil type characterized by average shear-wave velocities (Vs30) between 180 and 900 m/s. Damage results are obtained for a building typology representative for southern Spain and three height ranges (low, medium, high) indicating large differences in the derived MDR values for all topographic amplification models considered.

Keywords: topographic amplification, seismic damage, site effects, SELENA

1. Introduction

Studies on the phenomenon of topographic amplification of seismic waves date back to the early 1960s. Since then, many studies have revealed that topographic features such as slopes or ridges are able to amplify seismic ground motion and hence may increase the damage extent to buildings significantly. However, though topographic amplification can be considered as a well-investigated research field, it is still not addressed in the majority of international building design codes, and neither has been considered in any study or procedure for earthquake loss estimation (ELE) worldwide.

Topographic amplification effects were reported during the following earthquakes: 1909 Lambesc [1], 1985 Chile [2], 1987 Whittier Narrows [3], 1995 Aegeon [4] , 1999 Athens [5], 2003 Boumerdes [6], 2008 Achaia-Ilia [7], 2011 Christchurch [8] , 2015 Gorkha [9] , amongst others.

The amplification of seismic ground motion on hilltops and steep slopes is in general caused by the interaction between the incoming seismic waves and these geomorphical features (Fig.1). Many studies revealed that the impact of topographic amplification is maximum when the incident wavelengths (λ) are comparable with, or slightly shorter than the hill width and that a direct relationship exists between topographic amplification and the ratio between H/λ, where H is the slope height and λ is the wavelength of the input ground motion [15].

Quantifying the impact of topographic amplification on structural damage turns out to be difficult as in many cases it may not be possible to separate these effects from soil amplification, earthquake-triggered slope failure or an increased vulnerability of the structures. The latter is often due to the sloped terrain, which imposes strong irregularities to the building configurations and the fact that these buildings show significant design deficits since building codes are mainly focused on buildings located on flat terrain [17].

While slope failure effects can be more easily identified, it is particularly difficult to distinguish between soil and topographic amplification, especially when the topographic feature consists of sedimentary soil materials (e.g. soil slopes at river banks) or when rock slopes are covered by soft sedimentary layers. A theoretical approach to this problem was discussed by [19]who investigated topographic and site amplification separately in order to identify the contribution of both to the apparent amplification, i.e. the type of amplification commonly "(..) derived from field studies of topographic effects (following earthquakes) and which generally does not take into account site amplification due to the natural frequencies of the soil column behind the crest and/or beyond the toe of the slope." To follow this procedure, however, it would be required to have high-quality recordings at various recording sites within the slope as well as detailed knowledge of local geological and geometrical conditions, which is difficult to achieve.

The field of earthquake loss estimation (ELE) gained momentum in the late 1990s with the first release of the FEMA and NIBS HAZUS methodology [20].

ELE is concerned with predicting the likely consequences of an earthquake or its shaking effects on an individual or a group of physical assets (usually buildings, structures, infrastructure facilities). The aim of ELE usually goes beyond the sole estimation of physical damage, by including the prediction of direct social and economic losses, business disruption, number of displaced households and shelter requirements, or even volumes of debris [21]. In general, ELE studies can be conducted using various approaches of which the most common ones are the empirical (or statistical) approach and the more recent analytical (or theoretical) approach. Other ways to conduct ELE studies are based on a hybrid approach or they rely on expert opinion. The various approaches differ in principle in the way earthquake ground motion is represented and building vulnerability is treated [21].

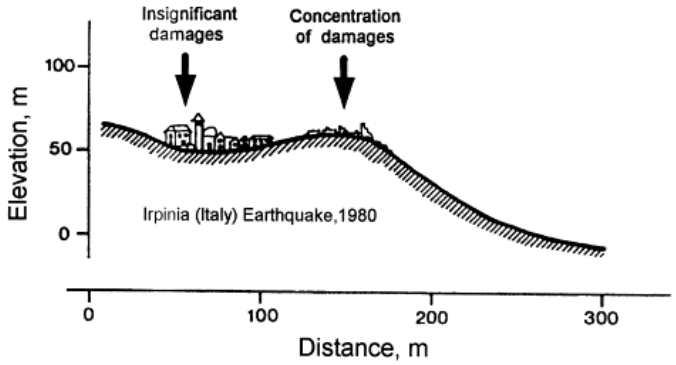

Fig. 1– Cartoon on effects of surface topography on damage distribution during the 1980 Irpinia (Italy) earthquake. Figure taken from [22].

With respect to providing the seismic ground-motion characteristics at the site of interest, i.e. at the locations of the physical asset under investigation, both seismic hazard and local geological subsoil conditions are considered. When focusing on ELE studies following the analytical approach, earthquake ground motion is usually provided in terms of a site-specific response spectrum that considers both the local hazard level at bedrock and the amplification potential of the local geological site conditions. However, with respect to the potentials for amplifying the seismic ground motion characteristics at a given site, the available procedures, software tools and conducted studies on ELE have been exclusively focusing on soil amplification, or more precisely, the amplification potential of the near-surface sedimentary layers. Even though it is widely accepted that, in addition to soil conditions, surface topography can have considerable influence on the frequency and amplitude characteristics of earthquake ground motion, this effect has been neglected in all of the existing ELE software tools, and neither do ELE studies in general consider this effect. Needless to say, the consideration of surface topography and its mapping and inclusion in ELE algorithms may only be important (and even worth the effort) in areas that are characterized by the presence of distinct topographic features, which by the way is often found in earthquake prone regions.

2. Topographic amplification in seismic design codes

As stated before, soil amplification factors are widely used in seismic design codes by adding a pre-defined factor to the elastic design spectrum. However, only a small number of seismic building design codes address topographic amplification, which may indicate that the scientific community has not yet come to a general consensus on this topic. The few exceptions of seismic building codes addressing topographic amplification are the French code AFPS 90 [23], the Italian code ICMS 2008 [24], [25], and Eurocode 8 [26]. In each of these provisions, topographic amplification is handled in a very simplified way with topographic amplification being solely represented by an amplification factor, which is to be added to the elastic design spectrum. Even if the Italian code ICMS specifies that this factor shall only be assigned to periods T between 0.1 and 0.5 s, the amplification factors are generally period independent, which means that the ordinates of the entire design spectrum are to be multiplied by the topographic amplification factor. This factor, referred to as τ or S_T, requires that the relief can be represented in a simplified 2D shape. Each of the respective design codes mention that irregular complex shapes will require specific studies.

In order to provide a comparison of these three codes in terms of topographic amplification, Table 1 (in combination with Fig.2) are summarizing the provisions for hilltops. Even if the computation of (maximum) topographic amplification factors can be considered straightforward and unambiguous in all codes, less explicit information is provided on affected areas, such as the segments of the topographic feature for which topographic amplification shall be applied, and how the transition of maximum topographic amplification factor to a factor of 1.0 shall be modelled.

Table 1 – Criteria for hilltops and their maximum topographic amplification factors as provided in the various seismic building codes.

Reference	Criteria				Maximum amplification	
	Slope height	Slope angle	Base width[2)]	Affected area	Amplification factor	Period range
AFPS 90	$H \geq 10$ *m*	$\alpha \geq 21.8$ % ($\tan\alpha \geq 0.4$)	*not specified*	a = *H*/3 for either side of the hill	$\tau = 1.00$ ($\alpha \leq 21.8°$) $\tau = 1+0.8\cdot(\tan\alpha-0.4)$ ($\alpha > 21.8°$) $\tau = 1.40$ ($\alpha > 42°$)	all periods
ICMS 2008	$H \geq 10$ m	$\alpha \geq 10°$	$L^* > 350$ m $L^* > 250$ m $L^* > 150$ m $L^* < 150$ m $l \geq 1/3 \cdot L^*$	"F_A shall be assigned to the entire crest *l*;" "from the crest along the slopes, F_A is to be scaled linearly until a value of 1 at the toe of each side."	max (F_A, S_T): $\ln(F_A) = 1.11 \cdot H/L^*$ $\ln(F_A) = 0.93 \cdot H/L^*$ $\ln(F_A) = 0.73 \cdot H/L^*$ $\ln(F_A) = 0.40 \cdot H/L^*$ $\ln(F_A) = 0.47 \cdot H/L^*$ $S_T = 1.2 - 1.4$	$T = 0.1 - 0.5$ *s*
EN 1998–5	$H \geq 30$ m	$\alpha \geq 15°$	*crest width << base width*	"(..) S_T should be used near the top of the slopes (..)" "(..) S_T to decrease as a linear function of the height (..) and to be unity at the base."	$S_T \geq 1.2$ ($\alpha \geq 15°$) $S_T \geq 1.4$ ($\alpha \geq 30°$)	all periods

[2)] in case of Italian code ICMS 2008, the base width of the topographic feature is marked as L^* since parameter *L* is generally used to define the half-width of the base of a hill, i.e. parameter L^* would correspond to 2*L*

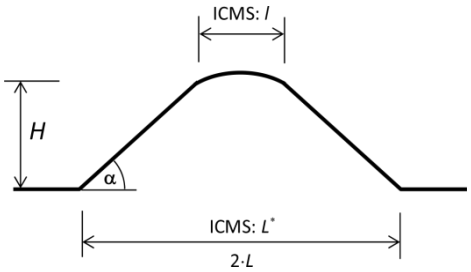

Fig. 2 – Description of topographic features (hilltop) as provided in various building codes.

Recently, [27] examined the role of topographic effects on the prediction of earthquake ground motion and its implication for seismic hazard analysis and seismic design. They propose to include an additional term in the existing ground motion prediction equations (GMPEs) to account for the effects of surface topography at a specific site. This factor is obtained from experimental and numerical analyses for the site of Narni. In particular with reference to the Italian building code, they concluded that national provisions are inadequate to define the seismic load at the top of ridges and crests.

Following a detailed review of the existing literature, [28] proposed a period-dependent topographic amplification relationship (including PGA) for sites at the top of a hill, which may be used in future ELE studies in hilly areas or regions characterized by sloped terrain. Therefore, based on this research, the goal of the present study is to investigate the sensitivity of the damage results (in terms of mean damage ratio – MDR) through a comparison when using the period-dependent topographic amplification relationship [28] and the simplified factors provided by Eurocode 8 (EC8) [26] and the Italian code [25].

3. Methodology

Seismic risk estimation is a tool to help public authorities not only to construct according to specific regulations but also to be prepared for emergency situations. This is the only way of reducing fatalities and losses being potentially caused by future seismic events.

In Spain, the low frequency of damaging earthquakes and the short social memory about their effects makes the population very vulnerable to this natural phenomenon. The M5.1, 2011 Lorca earthquake evidenced this situation. This event was the first one causing fatalities since the implementation of modern earthquake-resistant codes in Spain. Nine fatalities, thousands of displaced persons, significant damage to relatively recent buildings and elevated economic losses were the sad outcome of this event. In this case, failures on construction conception and the poor performance of non-structural elements were the main cause for this disaster.

The 1829 Torrevieja earthquake is known as one of the most damaging earthquakes in Spain and specifically the Alicante province. This event reached a macroseismic intensity X following the EMS-98 scale. The ground motion was highly amplified by the soft soils covering the areas closest to the Segura River causing significant structural damage in a wide area. 2965 buildings suffered extensive and complete damage, while 2396 buildings experienced moderate damage. With respect to the human losses, 389 persons died and 375 suffered injuries of moderate severity. [29] studied the seismic activity of the Bajo Segura fault zone and obtained that the maximum moment magnitudes range between 6.6 and 6.8 for individual fault segments and between 6.9 and 7.1 for a complete rupture of the Bajo Segura fault. Additionally, the focal depth was supposed to be shallow (approximately 5 km).

Based on this information, two cities (CTY1 and CTY2) located at 20 and 40 km from the Bajo Segura Fault (Fig.3) are chosen for the present study while three possible events of Mw 5.5, 6.0 and 6.5 are simulated. We have assumed that the buildings are located either on flat topography or a hill with a semilength of 150 m. The slope of the relief for both cities is ranging from 0 to 35 degrees (H/L from 0 to 0.7) and the soil conditions varies from rock (Vs30 = 900 m/s) to soft soil (Vs30 = 150 m/s) in case of flat terrain (H/L = 0) and Vs30 = 900 and 550 m/s in case of sloped terrain. Additionally, the ground-motion values are obtained using BEA [30] ground motion prediction equation. Fig.4 sketches all the possible combinations and solutions obtained.

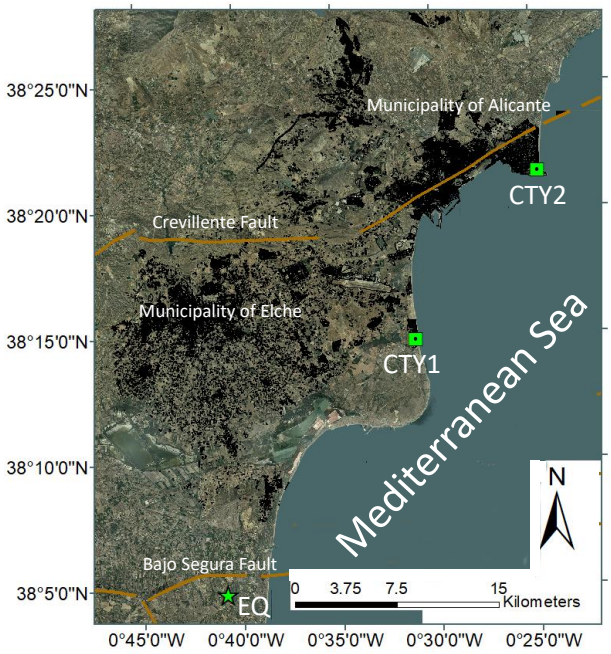

Fig. 3 – Geographical location of the simulated earthquake and the two cities.

The exposure in the city has been represented by the main structural typology, i.e. reinforced concrete frames with unreinforced masonry infills without seismic code design (named RC1-p low, medium and high rise) built between 1978 to 1996. The vulnerability of this building typology is represented by the curves provided by [31] named RC3-pre. For testing purposes, the number of building is fixed to 300, equally distributed among the low-, medium- and high-rise height classes.

The damage computation is done using the software SELENA [32] choosing the IDCM-method to compute the performance point and using three methodologies to account for topographic amplification: ICMS-2008 [33], EN1998-5 (EC8) [34] and period-dependent [36].

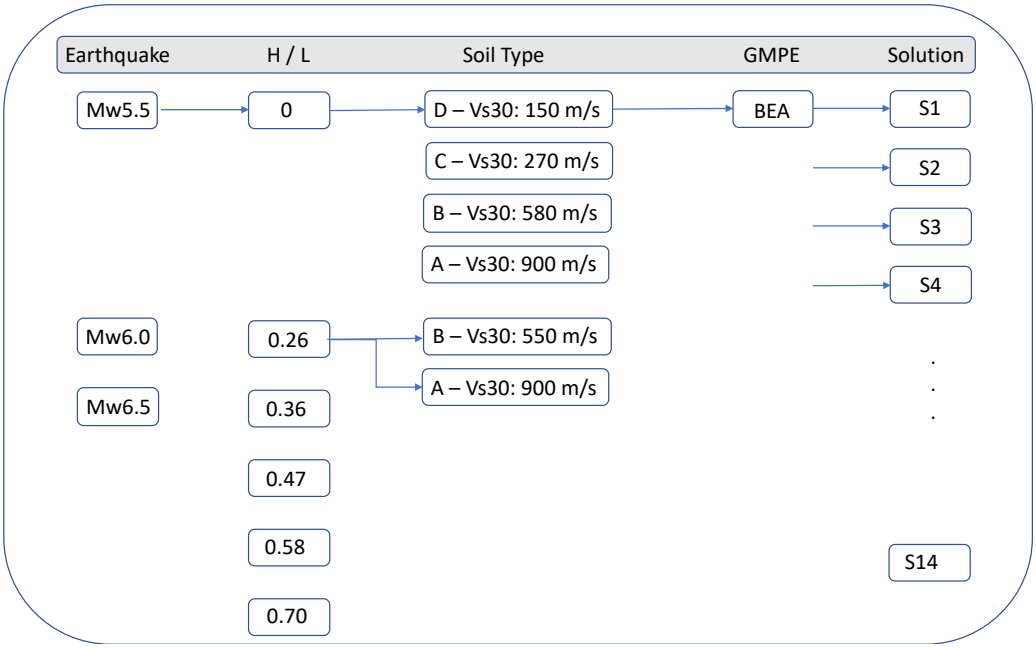

Fig. 4 – Scheme of the different MDR computations carried out

4. Results

Fig.5 shows the variability of Mean Damage Ratio (MDR) when using different soil types for both cities and assuming the occurrence of three earthquakes. As we can see, the MDR is higher for CTY1 (20 km from the rupture) and it is reduced by a factor of 2-3 for CTY2 (40 km from the rupture). Additionally, the highest damage appears for the very soft soil (D – 150 m/s) while it decreases from low-rise buildings to high-rise buildings. This behavior is different for the Mw6.5, when MDR increases from low-rise to high-rise buildings.

Fig.6 shows the MDR variability for a Mw5.5 event affecting buildings located on the top of a hill with slopes between 15 to 35 degrees. As we can see, the highest damage appears for CTY1. If the hill has a Vs30 of 900 m/s, the MDR is always lower than for a soil type B (550 m/s). Additionally, for slopes lower than 30º, the period-dependent relationship provides a higher MDR than EC8 or NTC2018. If the slope is higher or equal than 30º, EC8 provides the higher MDR. The damages are always higher for low-rise buildings than for the high-rise buildings. Finally, the period-dependent relationship shows a decreasing MDR when the slope angle increases.

A similar behavior can be observed in Fig.7 for a Mw 6.0 and finally Fig.8 shows the variability for a Mw6.5 event. Here we also can see how the MDR increases from low-rise to high-rise buildings in most of the cases.

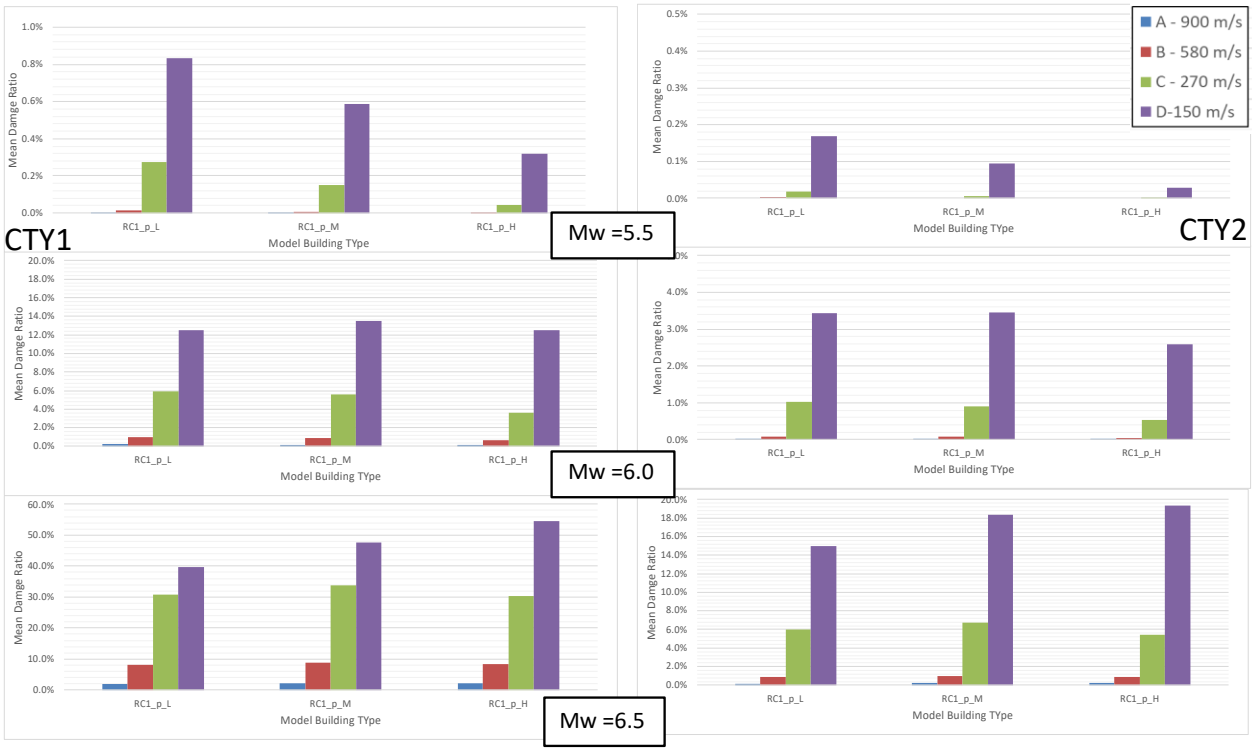

Fig. 5. MDR variability for different soil types.

5. Conclusions

In the present study, it is tried to quantify the variability of structural damage with respect to magnitude and distance of the damaging seismic event as well as site effects, i.e. soil and topographic amplification caused by soil class and slope angle, respectively. From the obtained results, the following observations can be made:

1. As many authors have stated before, structural damage is most sensitive to local geology (represented by soil class and hence average shear wave velocity Vs30). However, this is foremost true in case of flat terrain, i.e. when topography is not considered. As can be seen from Fig.5, the MDR values range from 2% to 40% for a magnitude 6.5 in CTY1 when varying between soil classes A to D. On the other hand, when varying the slope from 15º to 35º the MDR values never reach values greater or even 40%, while the differences between the results for the flattest and steepest slope are less than the differences observed for various soil classes.

2. Topographic amplification still has a significant effect on the predicted MDR, which is why it should be taken into consideration for earthquake loss estimation. As it can see from Fig.6 to 8, MDR can increase up to 25% for slopes with slope angles steeper than 25º.

3. Generally, the EC8 and NTC2018 models provide lower MDR values than the period-dependent relationship for slopes up to 25 degrees, while this trend is reversed for slopes steeper than 25 degrees. While both EC8 and NTC2018 models show similar trends in MDR for many of the investigated scenarios, the 25 degree slope can be considered as the case where the trend of MDR switches, i.e. larger MDR values for the period-dependent relationship for slopes flatter than 25 degrees and larger MDR values for the EC8 and NTC2018 models for slopes steeper than 25 degrees. This behavior, related with the change of the period of maximum amplification when the geometry of the relief varies, should be investigated more in future works.

4. The MDR values usually decrease from low-rise to high-rise height classes in case of the building typologies selected, independent of the chosen topographic amplification model. However, for the M6.5 scenario, the MDR is equal or slightly higher for medium-rise and even high-rise buildings.

Finally, this work shows the differences that can be found when using different topographic amplification relationships in ELE. Additionally, not always a higher slope can be related with a higher MDR (this is more evident in the period-dependent relationship). As the fragility functions used are those for regular buildings on flat terrain, it may happen that a higher seismic demand due to topography does not lead to a greater damage. In any case, this is something to be investigated in future works.

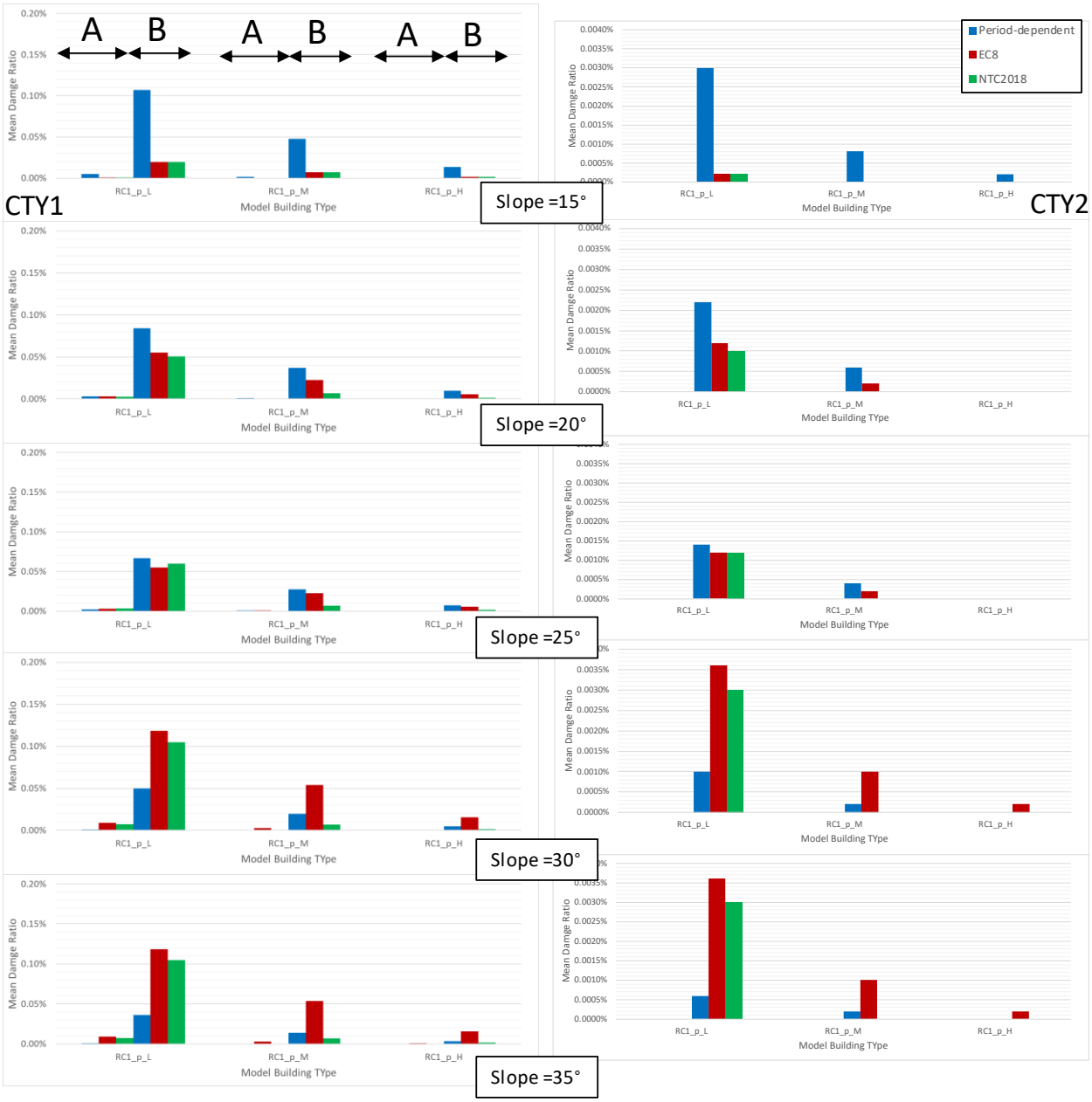

Fig. 6 – MDR for a scenario event of magnitude 5.5.

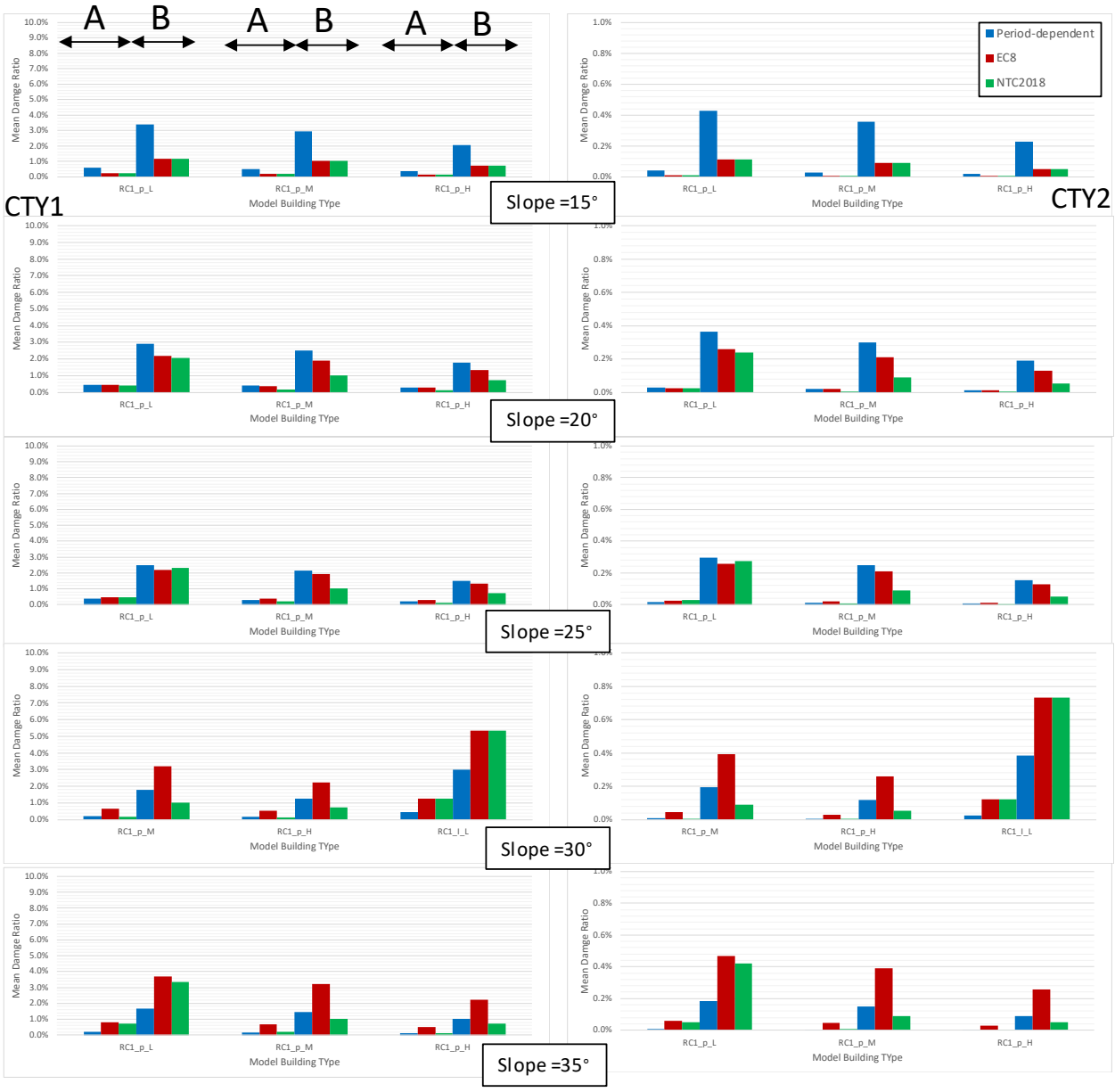

Fig. 7 – MDR for a scenario event of magnitude 6.0.

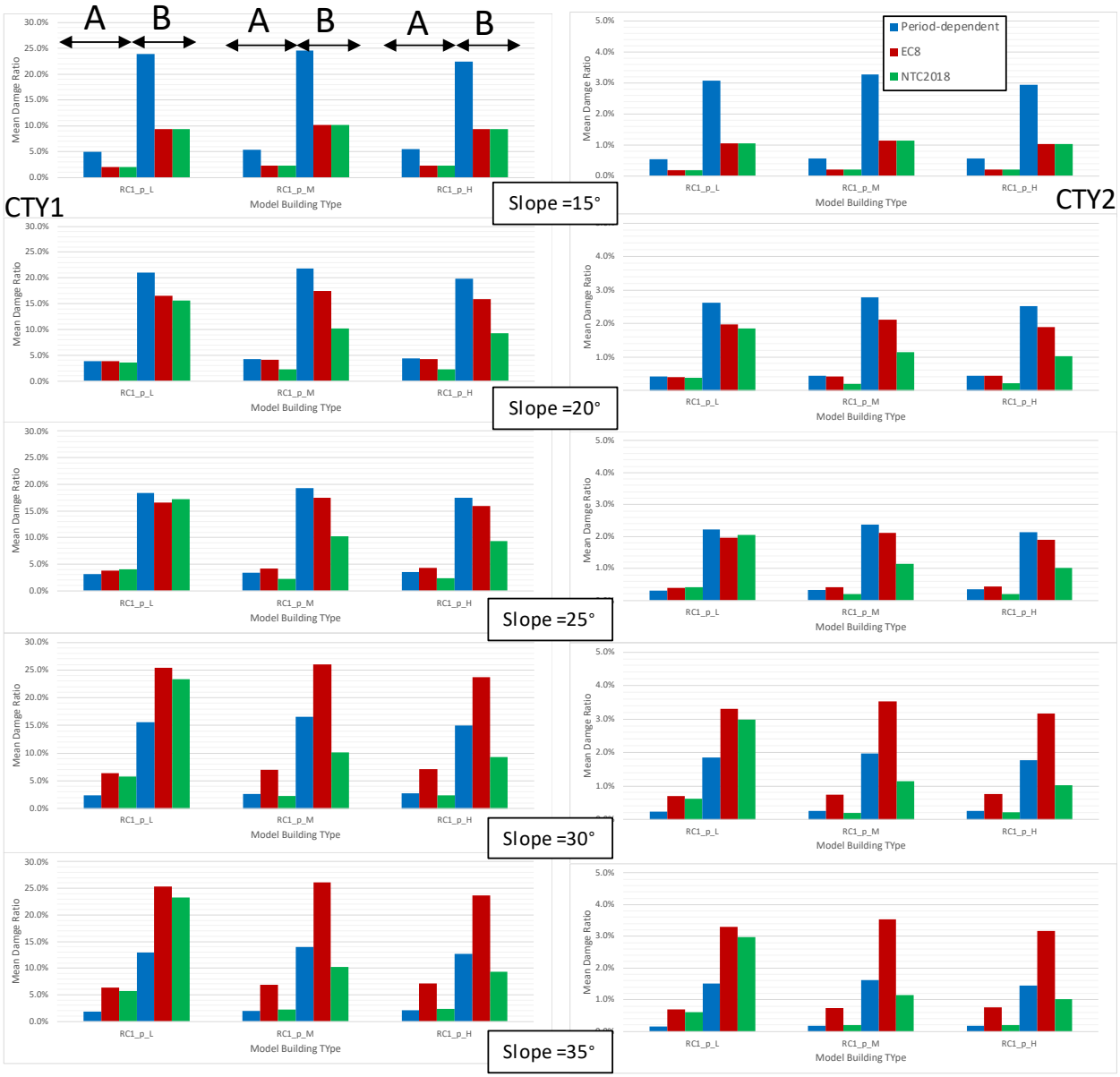

Fig. 8 – MDR for a scenario event of magnitude 6.5.

6. Acknowledgments

The research presented has been benefited from funding of the Ministerio de Economía, Industria y Competitividad through research project CGL2016-77688-R(AEI/FEDER,UE), the Generalitat Valenciana through the research project AICO/2016/098 with the collaboration and funding provided by Elche and Alicante municipalities.

7. References

[1] Levret A, Loup C, Goula X (1986): The Provence earthquake of June 11th, 1909 (France): New assessment of near-field effects. *Proc. 8th European Conference of Earthquake Engineering*, Lisbon, September 1986, Vol. 2, 4.2.79.

[2] Athanasopoulos, GA, Pelekis, PC, and Leonidou, EA (1999): Effects of surface topography on seismic ground response in the Egion (Greece) 15 June 1995 earthquake. *Soil Dynamics and Earthquake Engineering* **18** (2), 135–149.

[3] Çelebi M, Hanks T (1986): Unique site response conditions of two major earthquakes of 1985: Chile and Mexico. *Proceedings of the International Symposium of Engineering Geology Problems in Seismic Areas*, Bari, Italy, April 1986, Vol. IV.

[4] Bouckovalas GD, Gazetas G, Papadimitriou AG (1999): Geotechnical aspects of the 1995 Aegion, Greece, earthquake. *Proceedings 2nd international conference on geotechnical earthquake engineering*, Lisbon, June 1999, Vol. 2. Rotterdam: Balkema; pp.739–748.

[5] Gazetas G, Kallou PV, Psarropoulos PN (2002): Topography and soil effects in the Ms 5.9 Parnitha (Athens) earthquake: the case of Adames. *Natural Hazards* **27**, 133–169.

[6] Meslem A, Yamazaki F, Maruyama Y, Benouar D, Kibboua A, Mehani Y (2012): The Effects of Building Characteristics and Site Conditions on Damage Distribution in Boumerdes City after the 2003 Algeria Earthquake. *Earthquake Spectra* **28** (1), 185–216.

[7] Pelekis PC, Batilas AB, Vlachakis VS, Athanasopoulos G (2015): Topography Effects on Ground Response at the Town of Kato Achaia, in the Achaia-Ilia (Greece) Mw6. 4, 2008 Earthquake. *6th International Conference on Earthquake Geotechnical Engineering*, Christchurch, New Zealand, November 2015.

[8] Holden C, Kaiser A, Massey C (2014): Observations and analysis of topographic effects in the seismic response of the port hills following the 2011 Christchurch earthquake. *Proceedings of the Tenth U.S. National Conference on Earthquake Engineering, Frontiers of Earthquake Engineering*, July 21-25, Anchorage, Alaska.

[9] Wang F, Miyajima M, Dahal R, Timilsina M, Li T, Fujiu M, Kuwada Y, Zhao Q (2016): Effects of topographic and geological features on building damage caused by 2015.4.25 Mw7.8 Gorkha earthquake in Nepal: a preliminary investigation report. *Geoenvironmental Disasters* **3** (7), 1–17.

[10] Tripe R, Kontoe S, Wong TKC (2013): Slope topography effects on ground motion in the presence of deep soil layers. *Soil Dynamics and Earthquake Engineering*, **50**, 72–84.

[11] Singh Y, Lang DH, Narasimha DS (2015). Seismic risk assessment in hilly areas: case study of two cities in Indian Himalayas. *Proceedings of the SECED 2015 conference: earthquake risk and engineering towards a resilient world*, 9–10 July, Cambridge, UK.

[12] Federal Emergency Management Agency (1997): HAZUS®97 Earthquake Loss Estimation Methodology. *User Manual.* Federal Emergency Management Agency, Washington, D.C., United States, 197 pp.

[13] Lang DH (2004): *Damage potential of seismic ground motion considering local site effects.* PhD dissertation, Bauhaus-Universität Weimar, Institute of Structural Engineering, 294 pp., URL: http://e-pub.uni-weimar.de/opus4/files/88/Thesis_DHLang.pdf

[14] Castellani A, Chesi C, Peano A, Sardella L (1982): Seismic response of topographic irregularities. *Proceedings of soil dynamics and earthquake engineering conference*, Cakmak AS, Abdel-Ghaffar AM, Brebbia CA (eds), Southampton, July 1982, Balkema/Rotterdam, Vol. 1: 251–268.

[15] Association Française du Génie Parasismique (1990): *AFPS 90, Recommendations for the redaction of rules relative to the structures and installations built in regions prone to earthquakes.* French Association for Earthquake Engineering, 183 pp.

[16] Working Group ICMS (2008): Indirizzi e criteri per la microzonazione sismica. Grupo di lavoro "ICMS". *Conferenza delle Regioni e delle Province autonome*, Dipartimento della protezione civile, Roma, vol 3 e Dvd (in Italian).

[17] NTC2018 (2018): *Norme tecniche per le costruzioni 2018.* Il Ministro Delle Infrastrutture, Decreto 17 Gennaio 2018, 530 pp.

[18] CEN (2004): *EN 1998-5, Eurocode 8—design of structures for earthquake resistance, part 5: foundations, retaining structures and geotechnical aspects.* European Committee for Standardization, Brussels.

[19] Barani S, Massa M, Lovati S, Spallarossa D (2014): Effects of surface topography on ground shaking prediction: implications for seismic hazard analysis and recommendations for seismic design. Geophysical Journal International **197** (3), 1551–1565. https ://doi.org/10.1093/gji/ggu09 5

[20] Molina S, Lang DH, Singh Y, Meslem A (2019): A period-dependent topographic amplification model for earthquake loss estimation. *Bulletin of Earthquake Engineering*, 1–17. http://doi.org/10.1007/s10518-019-00608-1.

[21] Alfaro P, Bartolomé R, Borque MJ, Estevez A, García-Mayordomo J, García-Tortosa FJ, Gil AJ, Gràcia E, Iacono CL, Perea H (2012): The Bajo Segura Fault Zone: Active blind thrusting in the Eastern Betic Cordillera (SE Spain). *Journal of Iberian Geology*, **38** (1), 271–284.

[22] Boore DM, Stewart JP, Seyhan E, Atkinson GM (2014): NGA-West2 Equations for Predicting PGA, PGV, and 5% Damped PSA for Shallow Crustal Earthquakes. *Earthquake Spectra*, **30** (3), 1057–1085. http://doi.org/10.1193/070113EQS184M

[23] Lagomarsino S, Giovinazzi S (2006): Macroseismic and mechanical models for the vulnerability and damage assessment of current buildings. Bulletin of Earthquake Engineering, **4**, 415–443. doi: 0.1007/s10518-006-9024-z.

[24] Molina S, Lang DH, Lindholm CD (2010): SELENA - An open-source tool for seismic risk and loss assessment using a logic tree computation procedure. *Computers and Geosciences*, **36** (3), 257–269. http://doi.org/10.1016/j.cageo.2009.07.006.

